


TELEMETRY CASE REPORT

Open Access



Improving emergence location estimates for Argos pop-up transmitters

Casey L. Brown^{*} , Markus Horning and Amanda M. Bishop

Abstract

Background: Recent advances in satellite tagging technologies for marine animals have provided opportunities to investigate the spatial ecology of pelagic species including at-sea behavior and predator–prey interactions. Implantable Life History Transmitters (LHX tags) provide postmortem data on location and causes of mortalities from tagged individuals. Following a mortality event and extrusion of the tag from within an animal, varying amounts of time may elapse between the onset of satellite transmissions, the first successful uplinks to the Argos satellite system and the first location estimate obtained from multiple uplinks. Externally attached pop-up archival transmitters (PAT tags) also only commence transmissions following pre-programmed detachment from a host. The amount of delay for both types of tags may vary with programming, sea state (e.g., wind, waves, currents and tides) tag exposure and satellite coverage. Thus, actual emergence locations for LHX and other pop-up satellite transmitters are hard to accurately determine. Larger errors (~ 10–50 km) may be associated with emergence locations than the errors inherent in the Argos system. Here we present a new approach based on a time-reversed state-space model to improving emergence location estimates and quantifying their uncertainty for pop-up satellite transmitters, using data from 24 LHX tags deployed at known locations in the Gulf of Alaska.

Results: Between May and June 2017, we deployed 12 LHX tags in two locations in Resurrection Bay and 12 tags in two locations in Prince William Sound, Alaska. When tracking models included all successful uplinks that resulted in Argos locations immediately after deployments, the emergence location could be predicted to within 3 km, on average. However, increasing transmission delays up to 16 h progressively reduced the accuracy to 6–12 km, and for delays of 24 h or longer, the actual emergence locations were outside of the 95% isopleth of estimates.

Conclusions: Emergence locations for pop-up satellite transmitters can be estimated by a time-reversed state-space model. The area confined by 95% isopleth of model output is an effective way to characterize an emergence location with an associated uncertainty. Our findings illustrate the importance of programming tags to enhance satellite uplinks to provide immediate and high-quality locations.

Keywords: Pop-up archival transmitter, Life History Transmitter, PAT tag, LHX tag, Argos

Background

Over the past two decades, archival, delayed-transmission satellite telemetry transmitters have provided researchers with tools to examine the short- and long-term movement patterns, stock structure, habitat mapping and behavior of a wide variety of pelagic species [1–4]. In addition to fundamental spatial ecology questions, researchers are using pop-up archival transmitters

(PAT tags) to investigate post-release mortality rates from bycatch [5–7] and predation events [8–10]. External and internal PATs have benefits over implanted archival tags because data are retrieved via transmission through the Argos satellite system and the tags do not have to be retrieved to recover the data. Although PATs are very important research tools, their lower-than-expected uplink rates and sometimes incomplete data return postemergence remain problematic [9, 11]. Unavailable or low-quality location information at the end of an extended tracking period can make it difficult to model and refine movement paths. Thus, accurately defining an

*Correspondence: caseyb@alaskasealife.org
Alaska SeaLife Center, 301 Railway Ave, Seward, AK 99664, USA



emergence location has the potential of improving upon movement models.

For studies using PATs to analyze mortality events (e.g., predation, bycatch discard mortality), collecting spatially explicit data is required to accurately model spatial aspects of post-release survival. The quantification of predation, in particular, from many marine apex predators has been labeled “empirically intractable” [12]. The difficulty associated with identifying the role of predation on survival rates is largely due to the cryptic nature of pelagic predators and the effort associated with directly observing predatory behavior [10, 13, 14]. Rare, indirect predation rate estimates are often inferred at very different spatial and temporal scales and are subject to different sampling biases. These scaling constraints often result in large sample-size requirements and limited resolution with respect to resolving population trajectories and the factors driving them.

To overcome these limitations, Horning and Hill [15] developed an implantable Life History Transmitter (LHX tag) for applications in marine homeotherms. Classic telemetry applications on marine vertebrates rely primarily on externally attached, recoverable data loggers or transmitters. The retention for these devices is often limited to 1 year or less. Internal devices have been used successfully to monitor animals for periods beyond 1 year, but detection range, regional coverage and data recovery options have been limited [15]. Thus, LHX tags were designed to combine multi-year, life-long tag retention of internal archival devices, with global satellite-linked data recovery from tags after postmortem extrusion. LHX tags are intraperitoneally implanted under standard aseptic surgical conditions and gas anesthesia [16, 17]. LHX tags record data throughout the life of the host animal, and following death of the host, transmit previously stored information via satellite after the positively buoyant tags are liberated from decomposing, digested or dismembered carcasses. LHX tags provide the equivalent of spatially and temporally unrestricted known-fate (end of life) resight efforts and allow the at-sea detection and quantification of predation [18]. Mortality is determined from temperature data, and the resulting time stamp is included in data transmitted following tag emergence. Tag emergence following mortality is determined primarily via a light sensor [15]. In the case of predation, the timing of mortality and tag emergence usually coincide. The use of two LHX tags per animal increases data recovery probability and supports estimating event detection probability from the ratio of dual-tag data returns over single returns.

Results from deployments of dual LHX tags in 45 juveniles have provided the first direct, quantitative measure of predation by apex predators on an upper trophic-level

marine mesopredator, the Steller sea lion (*Eumetopias jubatus*) [8, 9, 18]. However, the accuracy of the initial emergence estimate (i.e., predation event location) was only coarsely estimated at 10–50 km [18, 19]. In most of these 45 sea lion deployments, tags were programmed to only commence transmissions at local noon. Furthermore, multiple successful uplinks within a single satellite pass are required to estimate a transmitter’s location. This resulted in lags between tag extrusion and the first calculated location estimate obtained from the Argos service provider ranging from 1 h to several days.

The objective of this study was to increase the accuracy and quantify uncertainty of the estimated position of initial tag emergence for PATs. To meet this objective, we deployed 24 LHX tags at the ocean surface at known, simulated emergence locations and developed analytical tools to generate emergence location estimates from Argos tracking data. Because the Argos system typically provides multiple sequential location estimates, often with increasing accuracy, we tested models that backtrack and extrapolate to an earlier time from the sequence of all locations available. We tested a continuous-time, state-space model in “reverse” to estimate the site in which we deployed our tags.

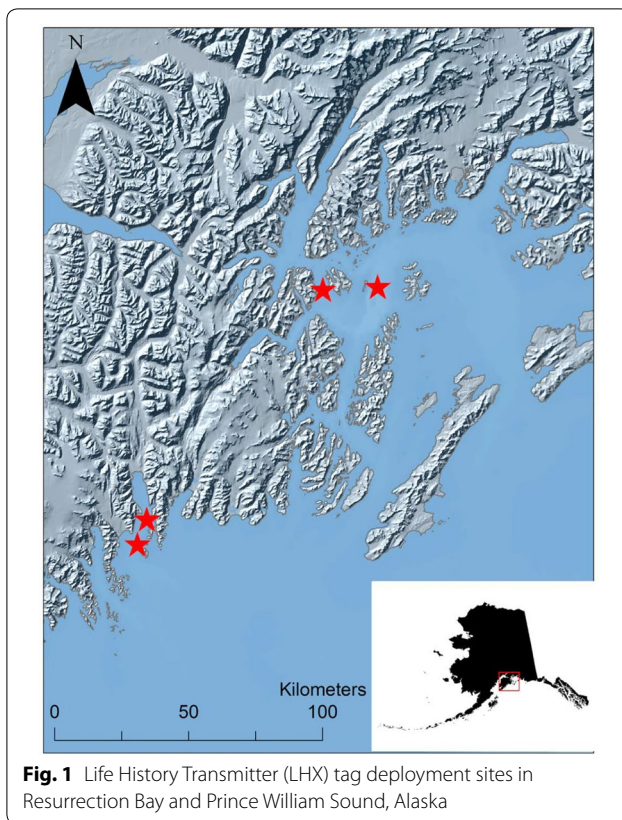
Methods

Tag deployment

LHX tags were programmed to transmit immediately and continuously for 10 days (or until battery depletion). Repetition period, which is the interval of time between two consecutive message dispatches, were programmed between 45 and 55(s). A 25 s rate was used on two tags to test whether faster rates would increase the likelihood of satellite uplinks, and provide a more accurate location estimate.

During May–June 2017, we deployed 24 tags at two sites in Resurrection Bay (Caines Head, 59.96°N 149.34°W; Calisto Head 59.88°N 149.43°W) and two sites in Prince William Sound, Alaska (Perry Passage 60.67°N 148.04°W; Lone Island 60.67°N 147.67°W). Both regions are characterized as sub-arctic fjord systems with direct connections to the oceanic waters of the Gulf of Alaska (Fig. 1). Both regions have mixed tides, with two high tides and two low tides with significantly different heights. However, depending on the location, tidal currents in Prince William Sound and Resurrection Bay can range from weak and variable (<0.5 knots) to moderate/strong (1–2 knots) [20].

Tags were deployed at the ocean surface and > 1 km from land to avoid tags prematurely washing up on shore. Winds were light (~ 1–5 knots) with small, non-breaking waves. Prior to operation, we used the position averaging feature on a hand-held GPS unit to record accurate



coordinates of the deployment location. Thus, in our testing here, the location of this simulated tag emergence was determined to an accuracy of 15 m. We used an Argos goniometer to find platforms ~1–3 h post-deployment to ensure tags were actively transmitting.

Model development

Tag transmissions received by Argos receivers aboard satellites in polar Low Earth Orbit are relayed via ground stations to a processing center operated by service provider CLS America, Inc. From the Doppler frequency shift measured in sequential uplinks received by any one satellite during a single pass, a likely location is calculated and assigned an accuracy in the form of one of 5 location classes (3, 2, 1, A and B), ranging from <150 m (LC 3) to >1.5 km (LC B). Processed location data were downloaded from the service provider via the Wildlife Computers Data Portal. These initial location estimates were then processed using several steps to remove low-accuracy locations and to interpolate points in time and space. We calculated an average daily drift rate starting at time of deployment until batteries shut down or tags washed ashore. To remove extreme outliers and meet normality assumptions for subsequent state-space models, we omitted all locations with LC Z (invalid location,

no error estimate). Tags' filtered paths were then interpolated into equal intervals (2 h, 12 locations per day) using a continuous-time, state-space model in the R (v3.4.0) package *crawl* [21]. This model is fit using the Kalman filter on a state-space version of the continuous-time stochastic movement process.

Because the emergence location is likely closest to the mortality event, we were most interested in accurately predicting this location. Since *crawl* models utilize Bayesian filters to estimate the current location conditional on locations from the past [22], output accuracy progressively increases as more locations are considered. Thus, we ran the model in reversed time to use all available spatial and location quality information: the final location obtained was reassigned to be the first location for the model, and all subsequent steps were backtracked in time. The first actual location estimate obtained by Argos was thus used as the last location in the model. Model output was then generated up to the time of emergence (or time of deployment for the 24 test tracks). In animal deployments, time of emergence is programmed (PATs) or determined by tags from sensor data and transmitted. This process was repeated 500 times per track, and locations were averaged across all simulations for a single track for each tag. To account for locations on land, we ran the final averaged path for each tag through *fixpath* in *crawl*, a function which moves points on land to the closest sea location along the path trajectory [21].

Model validation and error estimation

We used the estimated emergence location generated from the 500 simulated tracks to evaluate model accuracy. We used the point distances tool in the Geospatial Modeling Environment (GME v0.7.2.0) to calculate distances from each of the 500 estimated emergence locations and the true latitude and longitude for all tags associated with each actual tag deployment site. The distance between the *crawl*-estimated emergence locations and the actual deployment location from each site was used to calculate a mean distance and standard error (\pm SE) for each site. To test differences in location quality between tags programmed with fast and slow transmission rates (see Table 1), we compared the proportion of locations within the first 24 h that were assigned a LC 2 (<250–500 m) and 3 (<250).

Additionally, we produced a kernel density surface (KDS) from the concentration of estimated emergence locations (500 locations/tag) around each 30 m raster cell. We plotted the KDS as a series of isopleths that connected areas of equal occurrence. Isopleth values represent the boundary lines that contain a specified volume of points on a surface. Here, we use isopleth values to describe the likelihood of encountering the deployment

Table 1 Life History Transmitter (LHX) tag summary (n = 24)

Tag	Deployment site	Transmission rate (s)	Average daily drift (km)	First location and deployment distance (LC)	Prop. LC 2/3	# hours to first location	# hours to first LC 2/3
LHX692*	Caines Head	25	15	0.8 (2)	0.40	< 1	4
LHX699	Caines Head	46	12	3.1 (1)	0.20	2	2
LHX675	Caines Head	53	13	5.3 (A)	0.30	3	17
LHX695	Caines Head	47	14	6.2 (B)	0.10	3	6
LHX685**	Caines Head	56	11	2.1 (0)	0.20	< 1	19
LHX681	Caines Head	48	15	2.5 (0)	0.60	< 1	15
LHX673	Calisto Head	52	5	3.0 (B)	0.32	2	7
LHX693	Calisto Head	45	10	8.1 (A)	0.12	3	19
LHX810*	Calisto Head	26	6	5.2 (0)	0.70	2	2
LHX691**	Calisto Head	55	7	2.2 (3)	0.45	2	2
LHX676	Calisto Head	49	6	2.0 (A)	0.60	2	4
LHX686	Calisto Head	50	6	2.9 (B)	0.40	2	2
LHX680*	Lone Island	26	10	1.2 (0)	0.30	< 1	< 1
LHX698	Lone Island	45	7	2.9 (1)	0.20	< 1	5
LHX683	Lone Island	47	6	1.3 (0)	0.10	< 1	2
LHX690	Lone Island	49	8	3.7 (0)	0	< 1	4
LHX696**	Lone Island	51	10	1.8 (1)	0.20	< 1	2
LHX702	Lone Island	53	9	4.5 (A)	0.30	2	4
LHX674*	Perry Strait	25	16	2.1 (3)	0.50	< 1	< 1
LHX682	Perry Strait	46	20	3.1 (3)	0	< 1	< 1
LHX684	Perry Strait	48	21	4.5 (A)	0	< 1	3
LHX689	Perry Strait	50	25	15 (B)	0.10	5	24
LHX694	Perry Strait	52	26	3.0 (3)	0.25	1	1
LHX701**	Perry Strait	54	21	1.4 (3)	0.15	< 1	< 1

*Represents tags with "fast" transmission rate versus **tags with slow repetition rates. Proportion of location class (LC) 2/3 represents the proportion of location classes 2 (< 250–500 m) and 3 (< 250 m) within the first 24 h. The first location and deployment distance designates the distance between the first computed location we obtained via satellite and the deployment site along with the resulting location class

site in a particular area. We recorded the closest isopleth value to the deployment site locations. We characterized models as being accurate if deployment sites were within the 95th density isopleth. If deployment sites were outside of the 95th density isopleth, we deemed these models as inaccurate because 95% of generated emergence locations were isolated from the deployment site.

Due to the variability in time lags between mortality time stamps, emergence and the first Argos location estimate, we investigated the effects of LHX transmission delay on the emergence location estimate. We subsampled the original Argos-derived datasets, removing the first 8 h, 16 h, 24 h, 48 h, 72 h and 120 h of uplinked locations and reran the reverse models to produce estimated emergence locations. We used the timestamp at deployment to back-calculate the emergence location from *crawl* models. Again, we calculated the mean distances between the emergence location and the deployment sites (\pm SE) as well as nearest isopleth values from the plotted KDS.

Results

Twelve LHX tags were deployed at two locations in Resurrection Bay (Caines Head, $n=6$; Calisto Head, $n=6$) and twelve tags at two locations in Prince William Sound (Perry Passage, $n=6$; Lone Island, $n=6$). The mean number of days that tags uplinked in Resurrection Bay was 9 days (ranging from 3 to 13 days) and 7 days in Prince William Sound (ranging 3–10 days, Table 1). The distance that LHX tags drifted on the water surface from time of deployment to battery shutdown was highly variable across sites. Tags that were deployed in Resurrection Bay on average drifted daily 6.6 ± 1.1 km from Calisto Head (Table 1) and 13.3 ± 1.6 km from Caines Head. In Prince William Sound, tags deployed in Perry Passage drifted daily an average of 22 ± 3.4 km and 9 ± 3.4 km from Lone Island (Table 1). All tags generated at least one location fix with a LC class 2/3 in the first 24 h after deployment; however, tags that were programmed with the faster repetition rates had a greater overall proportion of high-quality location fixes than the tags with the

slower rate (Table 1). The time between deployment and the first computed locations obtained via satellite uplink ranged from 30 min to 5 h. The distance between the first obtained location of any class and the deployment sites ranged from 0.77 to 15 km (Table 1). For most tags, it took longer (1–24 h) to produce locations with a class 2/3 designation (Table 1).

Just as the distance of drift varied across sites, the mean distances between the estimated emergence location and the actual deployment sites were also highly variable. The most accurate emergence location estimates came from tags deployed at Calisto Head (2.3 ± 0.02 km) in Resurrection Bay and Lone Island (2.9 ± 0.03 km) in Prince William Sound (Table 2). Estimated emergence locations in Perry Passage gave the least accurate estimates (5.2 ± 0.06 km). Mean distances between estimates and actual locations in Perry Passage were almost twice as large as the mean distances from Caines Head, Calisto Head and Lone Island.

Models that used the full dataset of all locations (i.e., using all valid locations generated soon after deployment) generated the closest emergence location estimates to the actual deployment sites (Fig. 2). However, when initial Argos tracking locations were removed, simulating cases with delayed transmissions or uplinks, the mean distance between the estimated emergence locations and actual deployment locations increased substantially (Table 2). For example, when removing the first 24 h of location data, the distance between the estimated emergence locations and actual deployment sites increased three- to fourfold for all sites (Table 2). This trend was especially pronounced in Perry Passage, where the mean distance between estimated emergence locations and the deployment site increased to 50.9 ± 0.17 km after a 5 day (120-h) delay.

Nearest isopleth values generated from the full geospatial dataset ranged from 0.1 (Lone Island) to 0.6 (Caines Head) and confirmed that the inclusion of all data provided the most accurate emergence locations (Fig. 3). As

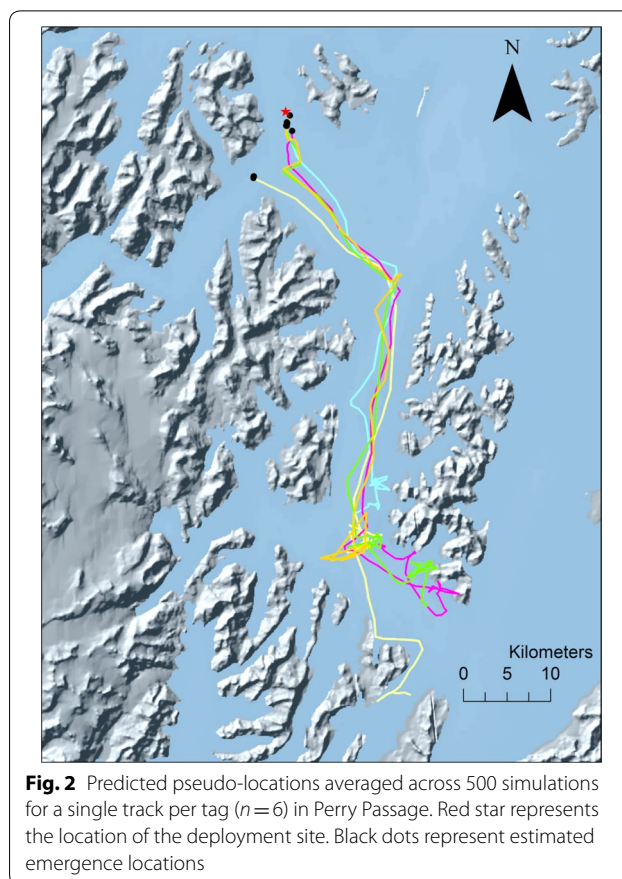


Fig. 2 Predicted pseudo-locations averaged across 500 simulations for a single track per tag ($n = 6$) in Perry Passage. Red star represents the location of the deployment site. Black dots represent estimated emergence locations

locations were removed from the dataset, the nearest isopleth value at deployment sites increased, suggesting a wider, less-concentrated spread of points (Fig. 4). Across all sites, the deployment location stayed within the 95% isopleth boundary for the first 16 h post-deployment (Table 3). In some cases, the deployment location was within the 95% isopleth value for 24 h post-deployment (Fig. 4). Isopleth values for Lone Island ranged from 0.1 to 0.7, suggesting these were the most accurate model predictions among sites.

Table 2 Mean distance (\pm SE) between *crawl*-estimated emergence locations and the actual deployment site

Dataset	Caines Head (km)	Calisto Head (km)	Perry Passage (km)	Lone Island (km)
All locations	2.9 ± 0.03	2.3 ± 0.02	2.6 ± 0.04	2.9 ± 0.03
8-h delay	5.1 ± 0.04	5.2 ± 0.03	3.5 ± 0.05	4.6 ± 0.04
16-h delay	11.8 ± 0.04	6.4 ± 0.04	10.6 ± 0.07	6.7 ± 0.06
24-h delay	12.8 ± 0.05	6.7 ± 0.04	20.5 ± 0.09	8.1 ± 0.08
48-h delay	15.9 ± 0.09	11.4 ± 0.04	36.8 ± 0.19	13.3 ± 0.15
72-h delay	14.4 ± 0.09	10.4 ± 0.05	49.7 ± 0.14	13.9 ± 0.16
120-h delay	17.8 ± 0.13	12.3 ± 0.13	50.9 ± 0.17	15.4 ± 0.23

“All locations” represent the full ARGOS location dataset, whereas 8-, 16-, 24-, 48-, 72- and 120-h delay represents a truncated dataset with removed locations to simulate transmission or uplink delays

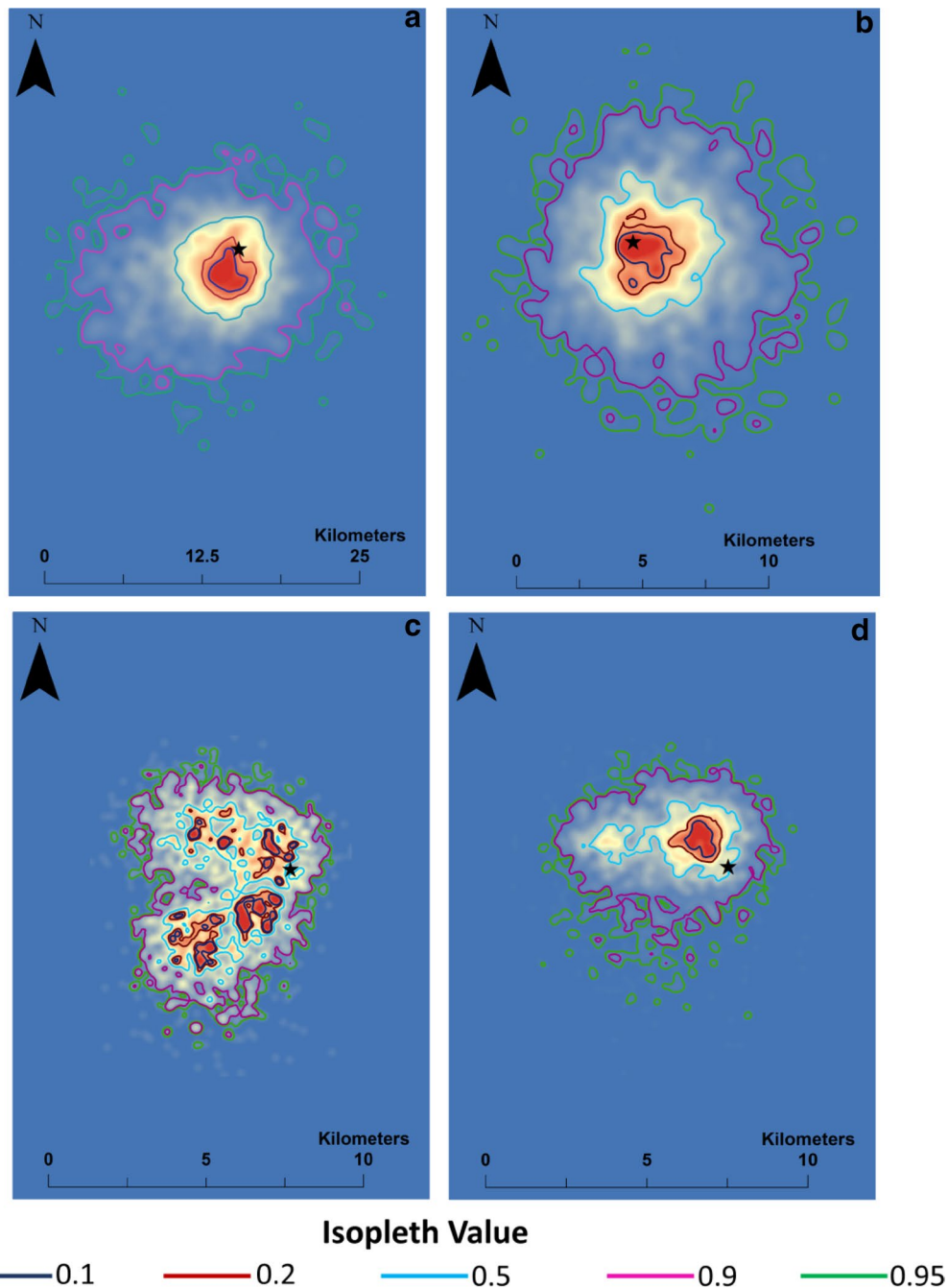


Fig. 3 Isopleth values generated from kernel density surface for *all* locations. **a** Perry Passage, **b** Lone Island, **c** Caines Head, **d** Calisto Head. Black stars represent the deployment site

Discussion

The application of LHX tags, in addition to modeling the spatial locations of mortality events, has advanced our ability to classify mortality by cause and location. We were able to apply a time-reversed state-space modeling technique to back-calculate an

initial, point-of-origin spatial location (the tag emergence location) and to provide an empirical error estimate, following varying lengths of transmission delay. Results from our models to backtrack spatial locations from implanted satellite telemetry tags revealed optimal accuracy of emergence location estimates of

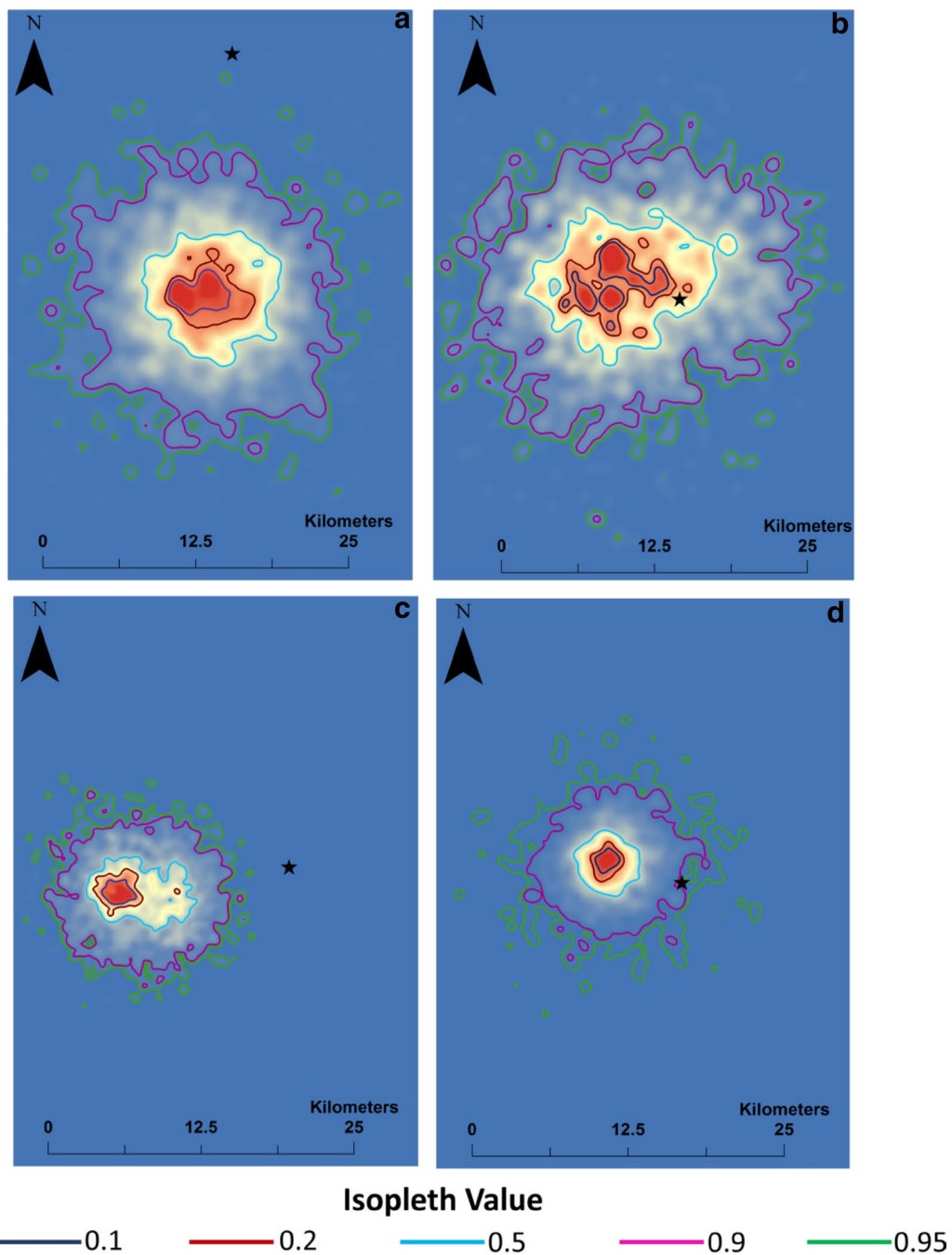


Fig. 4 Isopleth values generated from kernel density surface for a 24-hour delay. **a** Perry Passage, **b** Lone Island, **c** Caines Head, **d** Calisto Head. Black stars represent the deployment site

2.3–2.9 km, which on average, was an improvement over using the first location obtained (Table 1) and previous work that utilized the state-space models 95% confidence output [19]. These techniques worked especially well for datasets that began transmitting locations immediately at the ocean’s surface. For example, we

were able to generate a tag emergence estimate that was within 250 m of the Lone Island deployment site. Thus, our findings highlight the importance of optimizing tag programming to maximize probability of early uplinks in cases where research questions require immediate and high-quality locations of emergence.

Table 3 Nearest isopleth value to known deployment site

Dataset	Caines Head	Calisto Head	Perry Passage	Lone Island
All locations	0.60	0.50	0.20	0.10
8-h delay	0.80	0.80	0.70	0.70
16-h delay	0.90	0.90	0.90	0.50
24-h delay	< 0.95	0.90	< 0.95	0.40
48-h delay	< 0.95	< 0.95	< 0.95	0.40
72-h delay	< 0.95	< 0.95	< 0.95	0.40
120-h delay	< 0.95	< 0.95	< 0.95	0.30

"All locations" represent the full ARGOS location dataset, whereas 8-, 16-, 24-, 48-, 72- and 120-h delay represent a truncated dataset with removed locations to simulate transmission or uplink delays

However, transmission delays greater than 24 h substantially reduced accuracy of the emergence location estimates across three of 4 sites. We did find that all tags irrespective of the assigned repetition rates had at least one high-quality location class within 24 h of emergence which suggests that tags with slower transmission rates were able to provide a sufficient number of satellite uplinks. At time of deployment, we experienced light winds with little to no wave action, which likely maximized tag antenna exposure and the likelihood of transmissions being received by satellites. If successful uplinks are delayed > 16 h, the large gap in spatial information between the first location and the emergence site for *crawl* models will likely reduce the accuracy of the initial location estimates. To increase the likelihood of initiating satellite uplinks under more challenging wind and sea state conditions that may reduce antenna exposures, faster repetition rates are advisable. However, obtaining higher-resolution data usually compromises the longevity of the battery life. This trade-off might be ameliorated by programming tags to transmit rapidly during the first 12 h of emergence and then using a slower retransmit rate > 12 h.

Our results also provided insight into the surface movement patterns of implantable tags postmortem and the influence of environmental and oceanographic variables on location accuracy. Since tidal currents are typically highest at the mouth of most fjord systems [23], tags that were deployed at the heads of passages or fjords with large tidal fluxes were subject to greater surface drift over the life of the tag. For example, the waters surrounding Lone Island were classified as having "weak and variable" currents [20]. As a result, tags drifted an average of 9 km/day whereas tags from Perry Passage drifted over 20 km/day. The waters surrounding Perry Passage, in particular, can have strong surface currents especially in conjunction with high winds. Additionally, this correlates with

our data that showed emergence location estimates were more accurate for Lone Island tags than for Perry Passage tags. In addition to drift distance, ocean conditions at the time of the predation event will likely impact the spatial error associated with the emergence locations. Studies on marine mammals have found that spatial error is associated with surfacing behavior [24]. Given the small size of implantable satellite tags, it is likely that conditions at the ocean surface (e.g., wave height) will also affect the accuracy of the locations. To replicate conditions across sites, we only deployed tags in calmer conditions (winds speed: 1–5 knots; wave height 0–0.3 m). Thus, it is still unknown what effects rougher or choppy surface conditions will have on the accuracy of the emergence location.

Future applications should test the effects of tidal patterns, wave height and surface currents on the accuracy of emergence location estimates, especially in the case of long transmission delays. If regions have accurate and localized tide and current predictions, researchers could incorporate oceanographic drift models (e.g., Lagrangian drift models) into emergence location estimates. For example, recent research has used hydrodynamic drift models to predict mortality locations from sea turtle satellite-tag data [25, 26]. Experimental tests using drift models that account for wind and tide were also used to estimate at-sea mortality locations of cetaceans and resulted in differences in accuracy of approximately 30 km between true stranding locations and estimated locations [27]. However, the lack of baseline current and tidal data in coastal Alaska, especially at fine spatial scales, can make it challenging for researchers conducting such studies [28]. For example, we noticed that several LHX tags in Resurrection Bay spent several days floating in and out of small inlets and coves. This was likely due to localized, circuitous current pattern along the coastal coves versus the straight-line paths dictated by ebb and flood patterns within the fjord channels. As a result, the KDS generated from tags in Resurrection Bay revealed several localized hot spots (see Fig. 3), suggesting that the densities of initial location estimates were variable and spread over multiple areas. In the future, higher-resolution ocean models in conjunction with high-quality locations offer a promising alternative to backtrack and refine predation/pop-up locations.

Despite model accuracy decreasing with simulated transmission delays, our results have provided a direct, quantitative approach to estimate the location of predation events. Our empirical validation shows that for delays up to 16 h, actual emergence locations are included in the 95% isopleth of model outputs. Our results can be applied to other studies that use implanted satellite tags or pop-up archival tags. Quantifying the location of predation events can provide insight into how the spatial

scale of safe and risky areas influences the ability of prey to manage predation risk while foraging, moving and selecting habitats [29]. Predation risk mapping has been used in terrestrial ecology to investigate the influence of predation on resource selection decisions [30] and animal movement studies [31]. Although there is increasing evidence that marine animals modify their behavior under predation threat [32], few data or analyses exist showing how predators affect the movement of tracked marine animals. If predators are affecting the behavior of a tracked animal, especially in habitats where exposure to predation risk is persistent, results from habitat use studies may be incorrect or biased [33]. Finally, acquiring spatial information from mortality events may provide valuable information regarding the influence of predation on localized population declines. Recognizing the effects of predation on population recovery is essential for successful management and conservation of a range of threatened and endangered marine species. Thus, the application of LHX tags to classify mortality events in addition to modeling spatially explicit predation risk has potential to advance our ability to measure predation by apex marine predators on other upper trophic marine mammal species.

Conclusions

We were able to generate spatially explicit location estimates for simulated predation events by using a time-reversed state-space modeling technique that maximizes the use of all available location and quality information. In our empirical testing in four locations and for time delays up to 16 h postemergence, the actual points of origin were located within the 95% isopleth of model outputs. This suggests that the area confined by 95% isopleth of model output is an effective way to characterize an emergence location with an associated uncertainty.

Our results highlight that for studies prioritizing the emergence location, programming tags to optimize immediate, high-quality locations is critical. When using these methods, researchers should consider the amount of transmission delay as well as the quality (e.g., associated error) of the first few locations. Our findings also show that oceanographic conditions (e.g., current) may influence the accuracy of initial location estimates. In the future, researchers should consider testing how surface conditions can impact the accuracy of the initial transmission location. As it stands, these results provide valuable starting point to guide future research efforts seeking to identify the emergence location of pop-up satellite tags. The model can be applied more specifically to estimate the locations of predation or bycatch mortality events for a wide range of species including sea turtles, marine mammals and large pelagic fish.

Authors' contributions

MH built LHX tags with components supplied by Wildlife Computers, Inc., and tested and programmed LHX tags. CB analyzed the data and wrote the manuscript. AB and MH contributed to data interpretation and contributed to writing the manuscript. All authors read and approved the final manuscript.

Acknowledgements

We would like to thank Brandon Russel and Renae Sattler for assistance in the field.

Competing interests

The authors declare that they have no competing interests.

Consent for publication

Not applicable.

Ethics approval and consent to participate

Not applicable.

Funding

This research was supported by Award #1556495 of the National Science Foundation (U.S.).

Publisher's Note

Springer Nature remains neutral with regard to jurisdictional claims in published maps and institutional affiliations.

Received: 5 April 2018 Accepted: 25 February 2019

Published online: 11 March 2019

References

- Block BA, Dewar H, Farwell C, Prince ED. A new satellite technology for tracking the movements of Atlantic bluefin tuna. *Proc Natl Acad Sci*. 1998;95:9384–9.
- Boustany AM, Davis SF, Pyle P, Anderson SD, LeBoeuf BJ, Block BA. Satellite tagging: expanded niche for white sharks. *Nature*. 2002;412:35–6.
- Block BA, Teo SL, Walli A, Boustany A, Stokesbury MJ, Farwell CJ, Weng KC, Dewar H, Williams TD. Electronic tagging and population structure of Atlantic bluefin tuna. *Nature*. 2005;434:1121.
- Hazen EL, Maxwell SM, Bailey H, Bograd SJ, Hamann M, Gaspar P, Godley BJ, Shillinger GL. Ontogeny in marine tagging and tracking science: technologies and data gaps. *Mar Ecol Prog Ser*. 2012;457:221–40.
- Domeier ML, Dewar H. Post-release mortality rate of striped marlin (*Tetrapterus audax*) caught with recreational tackle. *Mar Freshw Res*. 2003;54:435–45.
- Horodysky AZ, Graves JE. Application of pop-up satellite archival tag technology to estimate postrelease survival of white marlin (*Tetrapterus albidus*) caught on circle and straight-shank ("J") hooks in the western North Atlantic recreational fish. *Fish Bull*. 2005;103:84–96.
- Campana SE, Joyce W, Manning MJ. Bycatch and discard mortality in commercially caught blue sharks *Prionace glauca* assessed using archival satellite pop-up tags. *Mar Ecol Prog Ser*. 2009;387:241–53.
- Horning M, Mellish JAE. Predation on an upper trophic marine predator, the Steller sea lion: evaluating high juvenile mortality in a density dependent conceptual framework. *PLoS ONE*. 2012;7:1.
- Horning M, Mellish JAE. In cold blood: evidence of Pacific sleeper shark (*Somniosus pacificus*) predation on Steller sea lions (*Eumetopias jubatus*) in the Gulf of Alaska. *Fish Bull*. 2014;112:297–311.
- Cosgrove R, Arregui I, Arrizabalaga H, Goni N, Neilson JD. Predation of pop-up satellite archival tagged albacore (*Thunnus alalunga*). *Fish Res*. 2015;162:48–52.
- Musly MK, Domeier ML, Nasby-Lucas N, Brill RW, McNaughton LM, Swimmer JY, Lutcavage MS, Wilson SG, Galuardi B, Liddle JB. Performance of pop-up satellite archival tags. *Mar Ecol Prog Ser*. 2011;433:1–28.

12. Williams TM, Estes JA, Doak DF, Springer AM. Killer Appetites: assessing the role of predators in ecological communities. *Ecology*. 2004;85:3373–84.
13. Hooker SK, Biuw M, McConnell BJ, Miller PJ, Sparling CE. Bio-logging science: logging and relaying physical and biological data using animal-attached tags. *Deep-Sea Res.* 2007;54:177–82.
14. Hussey NE, Kessel ST, Aarestrup K, Cooke SJ, Cowley PD, Fisk AT, Harcourt RG, Holland KN, Iverson SJ, Kocik JF, Flemming JEM. Aquatic animal telemetry: a panoramic window into the underwater world. *Science*. 2015;348:6240.
15. Horning M, Hill RD. Designing an archival satellite transmitter for life-long deployments on oceanic vertebrates: the Life History Transmitter. *IEEE J Ocean Eng.* 2005;30:807–17.
16. Horning M, Haulena M, Tuomi PA, Mellish JE. Intraperitoneal implantation of life-long telemetry transmitters in Otariids. *BMC Vet Res.* 2008;4:51.
17. Horning M, Haulena M, Rosenberg JF, Nordstrom C. Intraperitoneal implantation of life-long telemetry transmitters in three rehabilitated harbor seal pups. *BMC Vet Res.* 2017;13:139.
18. Horning M, Mellish JE. Spatially explicit detection of predation on individual pinnipeds from implanted post-mortem satellite data transmitters. *Endanger Species Res.* 2009;10:135–43.
19. Vazquez NA. Spatial and temporal distribution of juvenile Steller sea lion (*Eumetopias jubatus*) predation events in the Gulf of Alaska. M. Sc. Thesis, Oregon State University, Corvallis, OR; 2013.
20. National Ocean Services. Tide and Current Tables 2017. Pacific Coast of North America and Asia. <https://tidesandcurrents.noaa.gov>. Accessed 01 Dec 2017.
21. Johnson DS, London JM, Lea MA, Durban JW. Continuous-time correlated random walk model for animal telemetry data. *Ecology*. 2008;89:1208–15.
22. Särkkä S. Bayesian filtering and smoothing, vol. 3. Cambridge: Cambridge University Press; 2013.
23. Etherington LI, Hooge PN, Hooge ER, Hill DF. Oceanography of Glacier Bay, Alaska: implications for biological patterns in a glacial fjord estuary. *Estuaries Coasts.* 2007;30:927–44.
24. Costa DP, Robinson PW, Arnould JP, Harrison AL, Simmons SE, Hassrick JL, Hoskins AJ, Kirkman SP, Oosthuizen H, Villegas-Amtmann S, Crocker DE. Accuracy of ARGOS locations of Pinnipeds at-sea estimated using Fastloc GPS. *PLoS ONE*. 2010;5:e8677. <https://doi.org/10.1371/journal.pone.0008677>.
25. Nero RW, Cook M, Coleman AT, Solangi M, Hardy R. Using an ocean model to predict likely drift tracks of sea turtle carcasses in the north central Gulf of Mexico. *Endanger Species Res.* 2013;21:191–203.
26. Santos BS, Friedrichs MA, Rose SA, Barco SG, Kaplan DM. Likely locations of sea turtle stranding mortality using experimentally-calibrated, time and space-specific drift models. *Biol Conserv.* 2018;226:127–43.
27. Peltier H, Dabin W, Daniel P, Van Canneyt O, Dorémus G, Huon M, Ridoux V. The significance of stranding data as indicators of cetacean populations at sea: modelling the drift of cetacean carcasses. *Ecol Ind.* 2012;18:278–90.
28. Stabeno PJ, Bond NA, Hermann AJ, Kachel NB, Mordy CW, Overland JE. Meteorology and oceanography of the Northern Gulf of Alaska. *Cont Shelf Res.* 2004;24:859–97.
29. Brown JS, Kotler BP. Hazardous duty pay and the foraging cost of predation. *Ecol Lett.* 2004;7:999–1014.
30. Kauffman MJ, Varley N, Smith DW, Stahler DR, MacNulty DR, Boyce MS. Landscape heterogeneity shapes predation in a newly restored predator-prey system. *Ecol Lett.* 2007;10:690–700.
31. Thaker M, Vanak AT, Owen CR, Ogden MB, Niemann SM, Slotow R. Minimizing predation risk in a landscape of multiple predators: effects on the spatial distribution of African ungulates. *Ecology*. 2011;92:398–407.
32. Heithaus MR, Dill LM. Food availability and tiger shark predation risk influence bottlenose dolphin habitat use. *Ecology*. 2002;83:480–91.
33. Breed GA, Matthews CJ, Marcoux M, Higdon JW, LeBlanc B, Petersen SD, Orr J, Reinhart NR, Ferguson SH. Sustained disruption of narwhal habitat use and behavior in the presence of Arctic killer whales. *Proc Natl Acad Sci.* 2017;114:2628–33.

Ready to submit your research? Choose BMC and benefit from:

- fast, convenient online submission
- thorough peer review by experienced researchers in your field
- rapid publication on acceptance
- support for research data, including large and complex data types
- gold Open Access which fosters wider collaboration and increased citations
- maximum visibility for your research: over 100M website views per year

At BMC, research is always in progress.

Learn more biomedcentral.com/submissions

